The antitumour effect of galangin and luteolin with doxorubicin on chemically induced hepatocellular carcinoma in rats

Gamal Atwa[1], Gamal Omran[2], Atef Abd Elbaky[1], Tarek Okda[2]

[1]Department of Biochemistry, Faculty of Pharmacy, Port-Said University, Port-Said, Egypt
[2]Department of Biochemistry, Faculty of Pharmacy, Damanhur University, Damanhur, Egypt

Hepatocellular carcinoma (HCC), a highly malignant tumour with very high morbidity and mortality, remains the second cause of cancer-related deaths worldwide. Galangin is a naturally occurring flavonoid extracted from the propolis and root of Alpinia officinarum, which possesses antitumour efficacy, which has resulted in an increase in interest in related research. Additionally, galangin inhibits cell proliferation and induces apoptosis in several human malignancies. On the other hand, luteolin, a naturally occurring flavonoid found in a variety of edible plants, augments cytotoxicity in different cancer cells through the inhibition of cell-survival pathways and activation of apoptosis. Moreover, luteolin blocks the activity of anti-apoptotic Bcl-2 family members. The present study aimed to assess the antitumour effect of galangin and luteolin in combination and the antitumour effect of a combination of galangin and luteolin together with doxorubicin (DOX) in a chemically induced HCC rat model. Our analyses demonstrated that the combination treatment with galangin, luteolin, and DOX showed the greatest antineoplastic activity against HCC, which was observed by significant decreases in the levels of HCC markers, including serum α-fetoprotein-L3, and hepatic tissue expression of both glypican 3 and heat shock proteins. On the other hand, the hepatic tissue expression of caspase-3 was significantly increased. These results suggest that combination treatment with galangin and luteolin is a promising candidate for clinical use in HCC chemotherapy, especially when used in combination with DOX.

Key words: α-fetoprotein-L3, caspase-3, diethyl nitrosamine, galangin, hepatocellular carcinoma.

Contemp oncol (Pozn) 2021; 25 (3): 174–184
DOI: https://doi.org/10.5114/wo.2021.110048

Introduction

Hepatocellular carcinoma, one of the most significant cancers in humans, remains the second-most common cause of cancer-related deaths worldwide [1]. Conventional chemotherapy remains an important therapeutic approach for many malignancies although many patients experience severe toxicity. Various efforts have been made to enhance chemotherapeutic efficacy and decrease toxicity [2].

Therefore, in the past 2 decades, significant effort has been made to develop new drugs with improved specificity and efficacy toward hepatocellular carcinoma (HCC). Natural products play a vital role in the quest for promoting the specificity and potency of recent chemotherapeutic agents. Some examples include semisynthetic derivatives of taxanes and the flavone derivative flavopiridol; thus, identifying efficient plant-derived flavonoids with improved therapeutic effects and fewer side effects, which can be utilized in combination with currently available chemotherapeutic agents, may provide a significant approach in cancer treatment. Moreover, some flavonoids showed apparent anti-proliferative action against many multidrug-resistant tumour cell lines [3].

Galangin is a naturally occurring, strong flavonoid acquired from the propolis and root of *Alpinia officinarum*, a herb that has been used as a condiment and herbal remedy for various diseases in Asia for centuries [4]. Galangin is a flavonoid with anti-tumour activity, and it is considered a promising agent against liver cancer [5]. The biological actions of galangin include antimutagenic, anticlastogenic, antioxidative, metabolic enzyme modifying, and bactericidal effects [4]. Recent studies indicate that galangin possesses antitumour activity, which has attracted increasing interest. Specifically, galangin prevents cell proliferation and induces apoptosis in several human tumour cell lines including breast [6], pancreatic [7], gastric [8], and colon [9].

Luteolin is a naturally occurring flavonoid found in a variety of edible plants, which can induce cell cycle arrest or apoptosis in many human cancer cells [2]. In addition, luteolin induces cytotoxicity different cancer cells through inhibition of cell survival pathways and the induction of apoptotic pathways [10]. Combination therapy could kill malignant cells more efficiently by targeting multiple molecules and pathways together [11]. The main aims of combination research is to achieve a synergistic therapeutic effect using lower drug doses, and to lower or retard the development of resistance. Some flavonoids, alone or with other agents, have been shown to possess antineoplastic effects both in vitro and in vivo with little toxicity to normal cells, such as epithelial cells, myeloid cells, and peripheral blood [2]. In the present study, we aimed to assess the antineoplastic activity of galangin and luteolin as a combination when administered alone or togeth-

er with doxorubicin (DOX) in a rat model of chemically induced HCC.

Material and methods

Chemicals

Galangin, luteolin, and diethyl nitrosamine (DENA) were obtained from Sigma-Aldrich (USA). Doxorubicin (Adriamycin®) was obtained from Yick-Vic Chemicals (HK, China). All other chemicals and reagents were obtained from certified sources and were of analytical grade.

Animals and ethical approval

Adult male Wistar rats (150 g) were obtained from the animal colony of the Faculty of Medicine, Mansoura University, Egypt. All animals were housed under controlled environmental conditions (22 ± 2°C temperature, 50 ± 5% humidity, 12/12-hour light/dark cycle) and had free access to a typical grain diet and tap water. Animal care followed the guidelines of the National Institute of Health Guide for the Care and Use of Laboratory Animals and was approved by the Animal Ethics Committee (No. 518PB5) of the Faculty of Pharmacy in Damanhur University.

Experimental design

After a 2-week adaptation period, 75 healthy male rats were randomly categorized into 5 groups, with 15 animals in each group. Group I (negative control) included animals that received the vehicle solution comprising a mixture of 1% sodium carboxymethyl cellulose and 1% Tween 80, given daily by oral gavage during the experimental period. Groups II, III, IV, and V included animals that received a single intraperitoneal injection of DENA (200 mg/kg body weight) freshly dissolved in sterilized 0.9% saline. After 2 weeks, all animals in groups II-IV received a subcutaneous injection of CCl4 (3 mL/kg once weekly) for 6 weeks to enhance the carcinogenic effect of DENA [12]. The animals in group II (positive control) did not receive other treatments. The animals in group III were treated with DOX at a dose of 4 mg/kg body weight, once weekly for 4 weeks, administered intravenously via the tail vein [13]. The animals in group IV were treated for 4 weeks with a combination of galangin and luteolin (100 mg/kg body weight, daily) suspended in 0.5% (w/v) methylcellulose, administered by oral gavage [14, 15]. The animals in group V were treated with a combination of DOX, galangin, and luteolin using the doses and administration routes described for groups III and IV.

Serum specimen collection

Five millilitres of blood specimens were collected by cardiac puncture with the animals under ketamine anaesthesia (100 mg/kg/intraperitoneally) after a 12-hour fasting period following the final dose of treatment. The blood specimens were allowed to coagulate for 20 min, and serum was separated by centrifugation at 4000 rpm for 15 min at 4°C using a refrigerated centrifuge (Beckman model L3-50, USA) and stored at –80°C until the assessment of liver function markers.

Tissue specimen

The animals were euthanized by cervical dislocation. Next, livers were isolated, rinsed with cold phosphate-buffered saline (PBS), dried with filter paper, and split into 3 sections. The first section was stored at –80°C for analysis by real-time polymerase chain reaction (RT-PCR). The second section was homogenized in ice-cold PBS using a Potter-Elvehjem rotor-stator homogenizer (USA) to achieve 20% homogenate, which was centrifuged at 4000 rpm for 10 min at 4°C to remove debris. The third section was placed in 10% formalin for immunohistochemical analysis and histopathological examination.

Detection of glypican 3 and heat shock protein activity by real-time polymerase chain reaction

To achieve the maximum yield of intact RNA, one section of the liver was immediately harvested using the lysis buffer supplied in the GF-1 total RNA extraction kit (Vivantis Technologies, China) according to the manufacturer's instructions. All steps of total RNA extraction were completed on ice using ice-cold reagents. RNA concentrations were determined using a SPECTROstar Nano spectrometer (BMG Labtech, Germany). RNA quality was determined by measuring the 260/280 ratio. Single-stranded cDNA was created from 2 µg total RNA using the cDNA synthesis kit supplied in the 2-step RT-PCR kit (Vivantis Technologies) following the manufacturer's guidelines. The obtained cDNA was utilized to quantify target mRNA expression using RT-PCR amplification (Applied Biosystem step one, France) with a total reaction volume of 20 µL per well of an RT-PCR plate. The amplification reaction mixture contained 2 µL cDNA, 0.3 µL of each primer (10 µM), 10 µl SYBR Green universal master mix (Thermo Fisher Scientific, USA), and 7.4 µL DNase-free water. Real-time polymerase chain reaction conditions were as follows: 35 cycles of initial denaturation (95°C, 3 min), denaturation (95°C, 30 s), annealing (temperature dependent on specific gene, 30 s), and extension (72°C, 30 s) followed by final extension (72°C, 5 min). The primers were obtained from Vivantis Technologies (Malaysia), and the reference sequences obtained from the NCBI were applied to the design of the primers.

Glypican 3 (GPC3) forward Tm = 57.79°C: 5'-GTGCTGGAACGGACAAGAG-3'

GPC3 reverse Tm = 58.05°C: 5'-TTCTTCATCCCATTCCTTGC-3'

HSPs forward Tm = 55°C: 5'-TGTTAGCAGCCGGAATCAGT-3'

HSPs reverse Tm = 60°C: 5'-CTTGCTGAGCAGAGTTTTGAA-3'

β-actin forward Tm = 60°C: 5'-CTAAGGCCAACCGTGAAAAG-3'

β-actin reverse Tm = 60°C: 5'-TACATGGCTGGGGTGTTGA-3'

Real-time polymerase chain reaction data were evaluated to calculate fold changes and relative expression using the $2^{-\Delta\Delta CT}$ method by Livak [16]. β-actin was used as the endogenous reference gene.

Estimation of liver biomarkers

Serum alanine transaminase (ALT) and aspartate transaminase (AST) levels were determined according to the method by Reitman and Frankel [17]. Alkaline phosphatase (ALP) activity was measured according to the technique of Belfield and Goldberg [18]. Serum lev-

els of total bilirubin were determined according to the technique of Walters and Gerarde [19]. Serum α-fetoprotein-L3 (AFP-L3) levels were determined using an enzyme-linked immunosorbent assay kit from Glory Science (Hangzhou, China).

Estimation of oxidative stress biomarkers

Hepatic tissue homogenates were used to spectrophotometrically determine lipid peroxidation in liver tissues with thiobarbituric acid-reactive substance, and the results were expressed as malondialdehyde (MDA) equivalents using 1,1,3,3 tetramethoxypropane as the standard [20]. In addition, reduced glutathione (GSH) was spectrophotometrically measured in liver tissues using Ellman's method [21]. Superoxide dismutase (SOD) activity in liver tissues was estimated using the xanthine oxidase technique [22]. Nitric oxide (NO) was spectrophotometrically assayed in liver tissues by measuring its stable metabolites, in particular nitrite and nitrate [23].

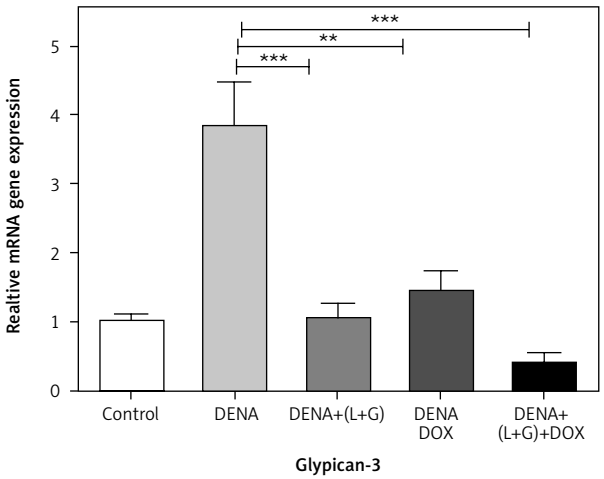

Fig. 1. Effect of galangin and luteolin compounds on GPC-3 mRNA level in liver tissue homogenates using real-time polymerase chain reaction

Results shown as means ± SEM (triplet)

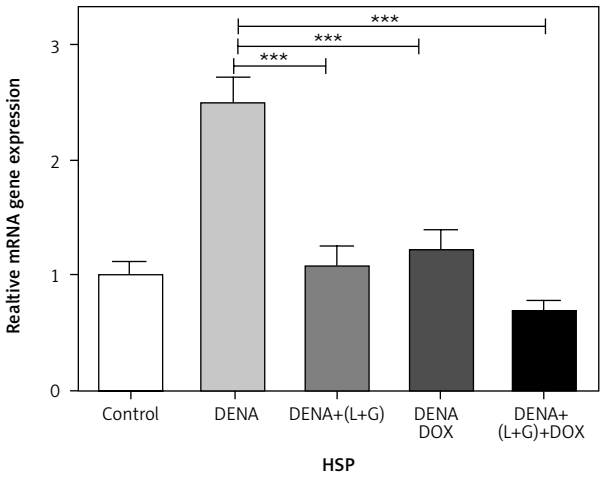

Fig 2. Effect of galangin and luteolin compounds on HSPs mRNA level in liver tissue homogenates using real-time polymerase chain reaction

Results shown as means ± SEM (triplet)

Immunohistochemical assessment

Immunohistological analysis of cleaved caspase-3 expression was performed on formalin-fixed, paraffin-embedded tissue. Briefly, 4–5 µm liver tissue sections on positively charged slides were deparaffinized in xylene, hydrated in a graded alcohol series, and pretreated for antigen retrieval in 10 mmol/L citrate buffer (pH 6.0) in a steamer at 98°C for 45 min. Immunohistochemical staining was performed by incubation of the slides with a polyclonal rabbit anti- cleaved caspase-3 antibody (catalogue number: ab2302) (1:1000 dilution). The slides were washed gently with PBS and incubated with a secondary antibody, followed by incubation with 3,3-diaminobenzidinetetrahydrochloride (DAB) for 10 min as the substrate chromogen solution. The slides were evaluated under a light microscope, and labelling index was calculated as the ratio of caspase-3-positive cells to the total number of cells. The number of labelled cells in immunostained sections was counted relative to 2000 cells [24, 25].

Histopathological assessment

The liver tissues were fixed in 10% formalin and dehydrated in a serial dilution of ethanol washes; the specimens were then cleared in xylene, embedded in paraffin at 56°C in a hot air oven for 24 hours, and sectioned at a thickness of 4–5 µm. The sections were stained with haematoxylin and eosin (H&E) and examined under a light microscope (Olympus, USA) by a histopathologist who was blinded to the treatment information [26].

Statistical analysis

Statistical analyses of data were performed using GraphPad Prism version 5.0 (GraphPad, San Diego, USA). Group comparisons were performed using analysis of variance followed by Tukey's t-test. The level of significance was set at a p-value of < 0.05, and all relevant results were graphically displayed as means ± standard error of the mean.

Results

Gene expression levels of glypican 3 by real-time polymerase chain reaction

The hepatic GPC3 gene expression was significantly increased in the DENA group compared with the control group ($p < 0.001$). However, the hepatic GPC3 gene expression was significantly decreased in the group treated with DOX and the group treated with the combination of galangin, luteolin, and DOX compared with DENA group ($p < 0.001$ and $p < 0.01$, respectively) (Fig. 1).

Gene expression of HSPs by real-time polymerase chain reaction

A significant increase in the hepatic HSPs gene expression was observed in the DENA group compared with the control group ($p < 0.001$). Moreover, combination treatment with galangin, luteolin, and DOX led to a significant decrease in the gene expression of HSPs ($p < 0.001$) compared with the DENA group ($p < 0.001$) (Fig. 2).

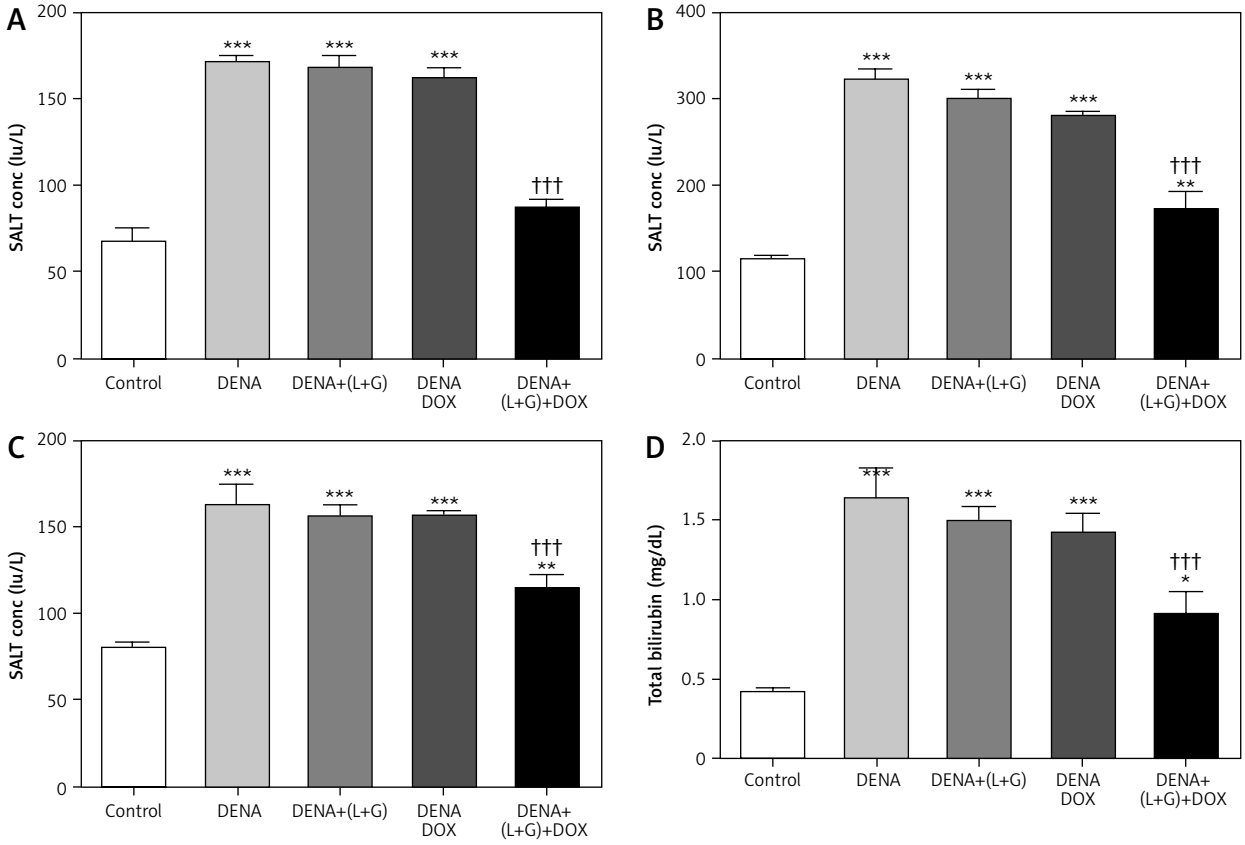

Fig. 3. Effect of galangin and luteolin compounds on the serum levels of alanine transaminase, aspartate transaminase, alkaline phosphatase, and total bilirubin

Data are presented as mean ± SEM (triplet).

**and † indicate significant changes from the control and diethyl nitrosamine groups, respectively*

Serum levels of alanine transaminase, aspartate transaminase, alkaline phosphatase, and total bilirubin

Our analyses revealed that the serum levels of ALT, ALP, AST, and total bilirubin were significantly increased in the DENA group ($p < 0.001$) compared with the control group. Additionally, the treatment with galangin plus luteolin or with DOX alone did not lead to changes in the serum levels of ALT, AST, ALP, and total bilirubin compared with the DENA group (positive control). Compared with the DENA group, the combination treatment with galangin, luteolin, and DOX was associated with significant decreases in the serum levels of ALT, ALP, AST, and total bilirubin ($p < 0.001$), Additionally the combination treatment with galangin, luteolin, and DOX was associated with significant increases in the serum levels of ALP ($p < 0.01$), AST ($p < 0.01$), and total bilirubin ($p < 0.05$) compared with the control group (Fig. 3).

Serum levels of α-fetoprotein-L3

Our assessment demonstrated that the serum AFP-L3 level was significantly increased compared with the control group ($p < 0.001$). Conversely, the treatment with galangin plus luteolin or with DOX alone did not lead to a change in the serum AFP-L3 levels compared with the DENA group. However, the combination treatment with galangin, luteolin, and DOX led to a significant decrease in the serum AFP-L3 level compared with the DENA group, although the serum AFP-L3 level in the combination treatment group was significantly higher than that in the control group (Fig. 4).

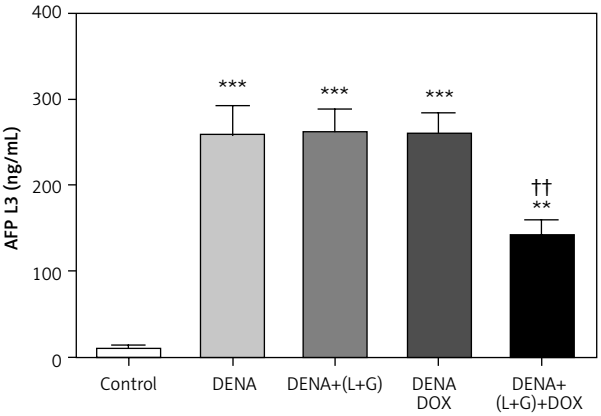

Fig. 4. The serum levels of α-fetoprotein-L3 as a circulating tumour marker of hepatocellular carcinoma in different groups

*Data shown as mean ± SEM (triplet). Data shown as mean ± SEM (triplet). *and † indicate significant changes from the control and diethyl nitrosamine groups, respectively*

Hepatic glutathione, superoxide dismutase, nitric oxide, and malondialdehyde content

Our assessment of the hepatic tissue revealed that the hepatic tissue levels of GSH and SOD were significantly

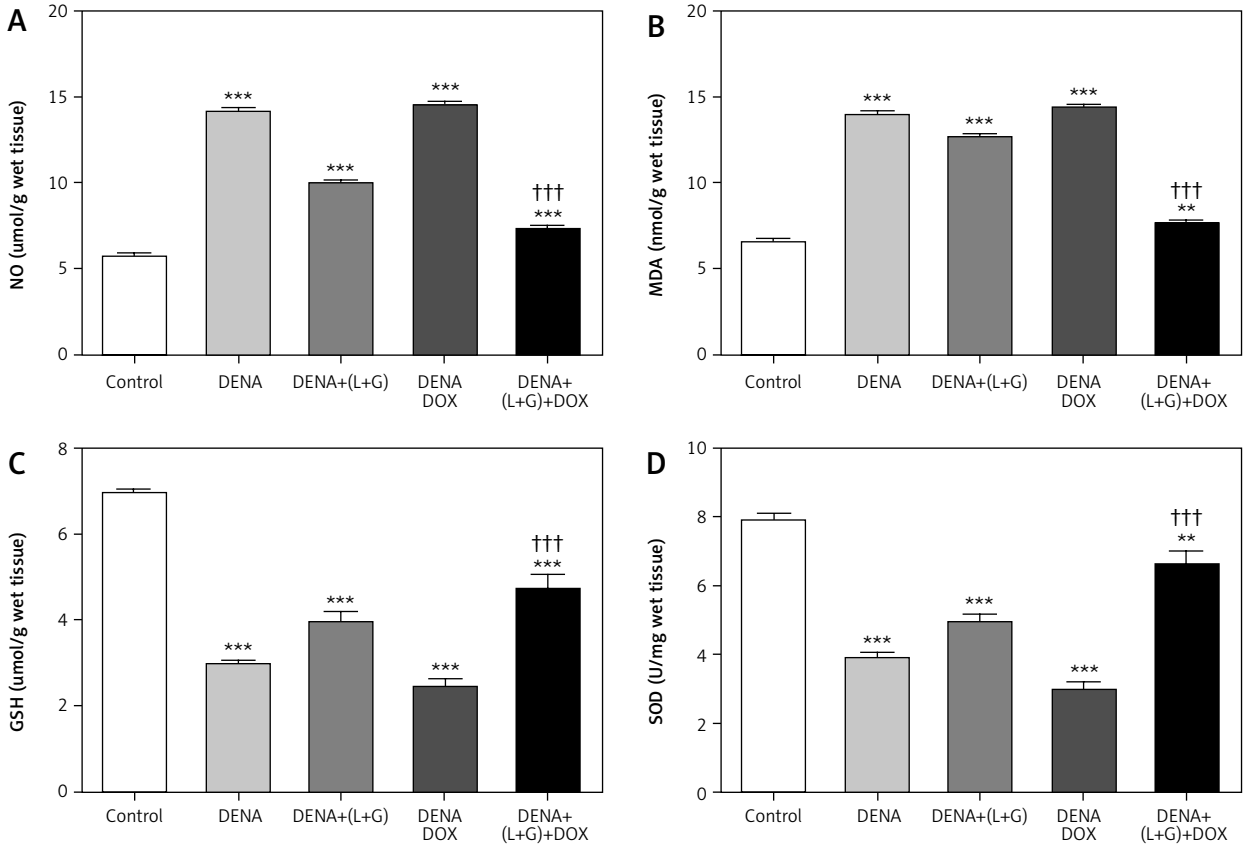

Fig. 5. Effect of galangin and luteolin compounds on levels of the hepatic content of nitric oxide, malondialdehyde, glutathione, and superoxide dismutase

Data are presented as mean ± SEM (triplet). Data shown as mean ± SEM (triplet).
** and † indicate significant changes from the control and diethyl nitrosamine groups, respectively*

decreased in the DENA group ($p < 0.001$) compared with the control group. In addition, the treatment with galangin plus luteolin or with DOX alone did not affect the hepatic tissue GSH and SOD content compared with the DENA group (positive control). Conversely, compared with the DENA group, the combination treatment with galangin, luteolin, and DOX led to significant increases in the hepatic tissue levels of GSH and SOD ($p < 0.001$). Additionally, the combination treatment with galangin, luteolin, and DOX was associated with significant decreases in the hepatic tissue levels of GSH ($p < 0.001$) and SOD ($p < 0.01$) compared with the control group (Fig. 5).

We also found significant increases in the hepatic tissue NO and MDA content in the DENA group ($p < 0.001$) compared with the control group. Likewise, the treatment with galangin plus luteolin or with DOX alone did not change the hepatic tissue NO and MDA content compared with the DENA group (positive control). In contrast, compared with the DENA group, the combination treatment with galangin, luteolin, and DOX led to significant reductions in the hepatic tissue NO and MDA content, Additionally, the combination treatment with galangin, luteolin, and DOX was associated with significant increase in the hepatic tissue content of NO ($p < 0.001$) and MDA ($p < 0.01$) compared with the control group (Fig. 5).

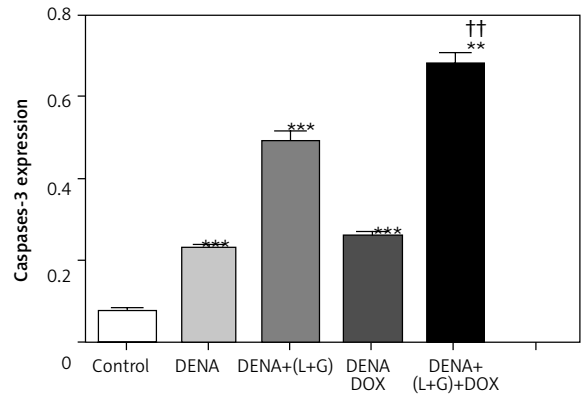

Fig. 6. Effect of galangin and luteolin on the hepatic cleaved caspase-3 expression by immunohistochemical analysis

Data shown as mean ± SEM (triplet)

Assessment of hepatic expression of cleaved caspase-3 by immunohistochemical analysis

We next determined changes in the hepatic cleaved caspase-3 expression using the labelling index and found that the hepatic cleaved caspase-3 expression was significantly increased in the DENA group ($p < 0.001$) compared with the control group. Furthermore, the combination treatment with galangin, luteolin, and DOX led to a significant increase in the hepatic cleaved caspase-3 expression ($p < 0.001$) (Fig. 6, 7). Regarding the proliferation of tumour cells demonstrated by

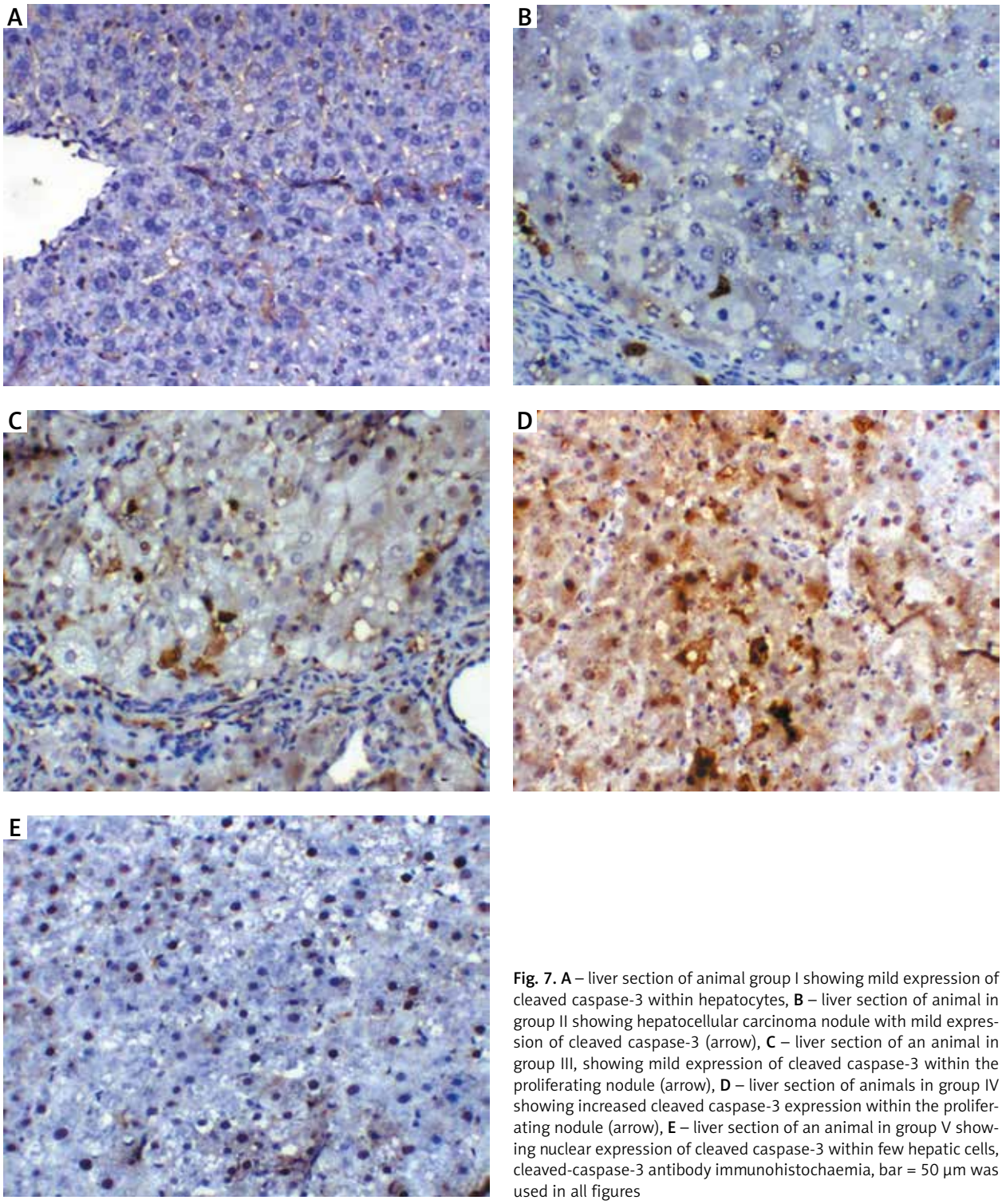

Fig. 7. A – liver section of animal group I showing mild expression of cleaved caspase-3 within hepatocytes, **B** – liver section of animal in group II showing hepatocellular carcinoma nodule with mild expression of cleaved caspase-3 (arrow), **C** – liver section of an animal in group III, showing mild expression of cleaved caspase-3 within the proliferating nodule (arrow), **D** – liver section of animals in group IV showing increased cleaved caspase-3 expression within the proliferating nodule (arrow), **E** – liver section of an animal in group V showing nuclear expression of cleaved caspase-3 within few hepatic cells, cleaved-caspase-3 antibody immunohistochaemia, bar = 50 µm was used in all figures

routine histology, the tumour cells showed a marked increase of proliferation activity with decreased apoptosis and necrosis within the tumour mass. We could not to proliferation marker within this time due to circumstances of the Covid-19 pandemic.

Histopathological examination

Photomicrograph A of Figure 8 shows a liver section from a normal adult male albino rat that underwent a sham operation, which shows normal hepatocytes arranged in cords around the central vein (arrow; haematoxylin and eosin [H&E] staining; scale bar, 100 µm). The photomicrograph B in Figure 8 shows a liver section from an adult male albino rat treated with DENA and demonstrating an HCC nodule not treated (arrowheads indicate nodule border) with hyperplastic atypical hepatocytes (arrow) (H&E staining; scale bar, 100 µm). Additionally, photomicrograph C in Figure 8 shows a liver section from an adult male albino rat exposed to DENA and DOX; the image shows an HCC nodule comprising thick hepatic trabeculae

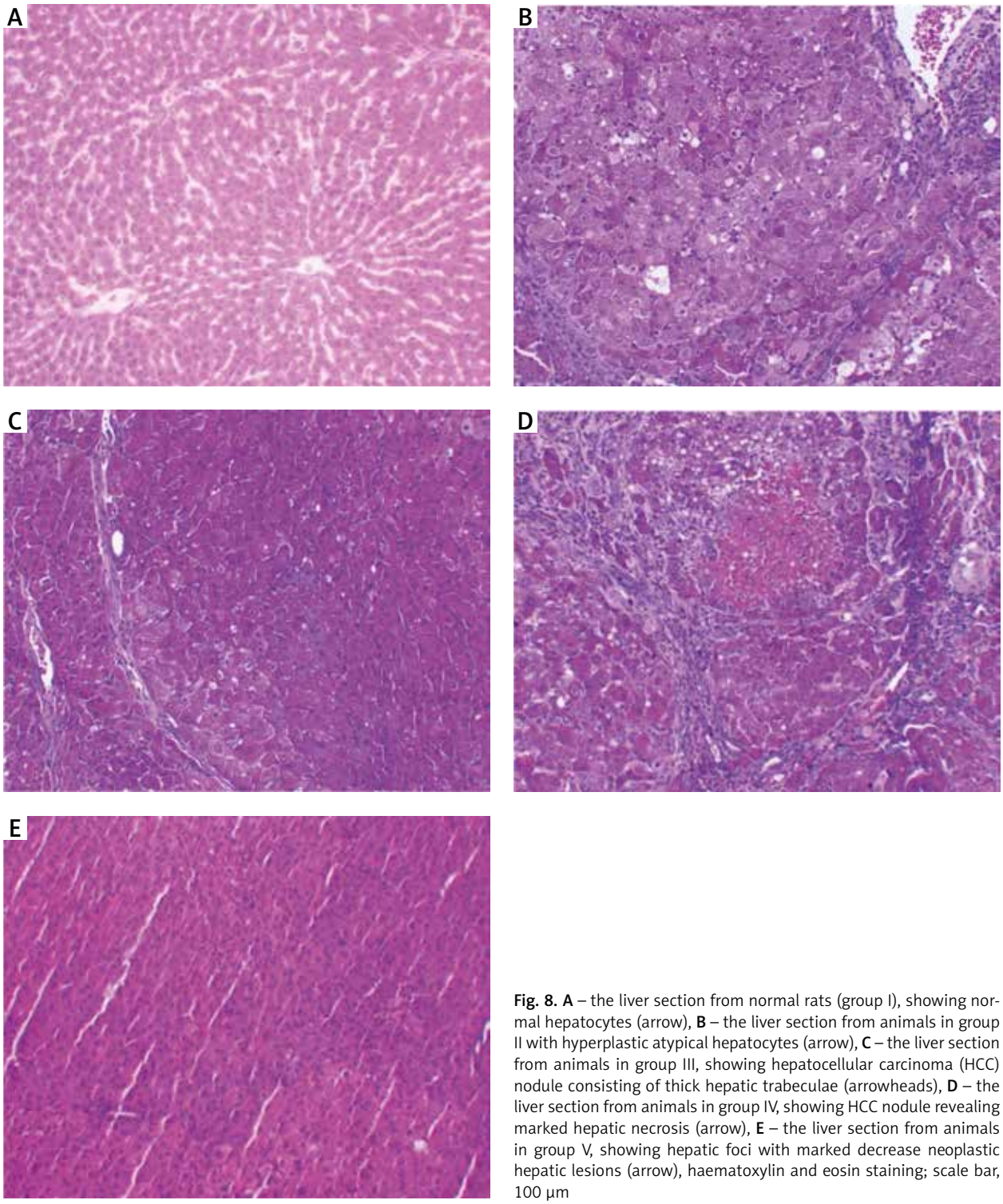

Fig. 8. A – the liver section from normal rats (group I), showing normal hepatocytes (arrow), **B** – the liver section from animals in group II with hyperplastic atypical hepatocytes (arrow), **C** – the liver section from animals in group III, showing hepatocellular carcinoma (HCC) nodule consisting of thick hepatic trabeculae (arrowheads), **D** – the liver section from animals in group IV, showing HCC nodule revealing marked hepatic necrosis (arrow), **E** – the liver section from animals in group V, showing hepatic foci with marked decrease neoplastic hepatic lesions (arrow), haematoxylin and eosin staining; scale bar, 100 µm

associated with marginal cytoplasmic atypia (arrowheads indicate nodule border; H&E staining; scale bar, 100 µm. Furthermore, photomicrograph D in Figure 8 shows a liver section from an adult male albino rat treated with a combination of DENA, galangin, and luteolin. The image shows an HCC nodule with marked hepatic necrosis (arrow; H&E staining; scale bar, 100 µm). Finally, photomicrograph E in Figure 8 shows a liver section from an adult male albino rat treated with a combination of DENA, DOX, galangin, and luteolin. The image shows hepatic foci with a marked decrease in neoplastic hepatic lesions with a small number of hepatic adenomas (arrow indicates normal hepatocytes; H&E staining; scale bar, 100 µm) (Fig. 8).

Discussion

Hepatocellular carcinoma is highly prevalent cancer. The utility of chemotherapy, albeit a popular therapeutic strategy after surgery for HCC, has been restricted because of its toxicity to normal tissues. Thus, the development of novel anticancer drugs that are nontoxic to nor-

mal tissues is important. Products from natural sources have been used to inhibit cancer for centuries and are thus envisioned as safer alternatives to their chemical counterparts [27].

The present study examined the in vivo effects of galangin plus luteolin, either alone or in combination with DOX, on HCC. The treatment of sus scrofa with 15 mg/kg DENA weekly produces a model for hepatic angiosarcoma that helps to discover new mechanisms of primary hepatic angiosarcoma and encourages treatment [28]. In the present study, liver integrity was estimated by measuring the serum levels of ALT, ALP, AST, and total bilirubin. Our analyses indicated that the levels of these liver biomarkers were elevated in the presence of HCC. Furthermore, the treatment with galangin plus luteolin or with DOX alone led to minimal improvement in these liver function biomarkers, which however exhibited significant improvements in the animals treated with the combination of galangin, luteolin, and DOX. These results are in agreement with a previous study [29]. Serum total AFP is a commonly used serological tumour biomarker for HCC because its serum levels are rapidly elevated in patients with HCC. However, serum total AFP has a limited specificity and sensitivity (25–60%) for predicting HCC [30]. Conversely, AFP-L3 has higher sensitivity as a serological marker for the diagnosis of HCC. In addition, AFP-L3 can be used in the monitoring of disease prognosis. The Food and Drug Administration has approved the use of AFP-L3 as an early diagnostic marker for HCC, with 10% of total AFP content as a positive crucial value because this ratio elucidates an incidence of over 95% for HCC [31].

The results of the present experimental study revealed that the serum AFP-L3 levels were significantly increased in the DENA group compared with the control group, and that the treatment with galangin plus luteolin or with DOX alone did not lead to a significant improvement in serum AFP-L3 levels. However, our results showing that the combination treatment with galangin, luteolin, and DOX significantly improved the serum AFP-L3 levels ($p < 0.05$) are in agreement with a previous study, which reported that the AFP-L3 fraction was more sensitive than AFP for small-sized or early-stage HCC. In addition, AFP-L3 can be detected in the serum 9–12 months before the detection of tissue lesions by screening. Finally, AFP-L3 can be used to determine disease prognosis [31].

We also found that the hepatic cleaved caspase-3 was significantly increased in the DENA group ($p < 0.001$) compared with the control group. Similarly, the caspase-3 expression was significantly increased ($p < 0.001$) after the combination treatment with galangin, luteolin, and DOX. These results are in agreement with another study which reported that luteolin demonstrated a significant induction in caspase-3, the executioner protease of apoptosis, in immortalized human hepatoma cell lines [32].

Furthermore, these results are in agreement with a study which reported that combination treatment with galangin and phytochemical agents such as berberine led to a synergistic suppression of both growth and tumour size in oesophageal cancer via the induction of cell cycle arrest and apoptosis without the induction of toxicity in vivo and in vitro [29].

Glypican 3 is a cell surface oncofoetal proteoglycan that is anchored by glycosyl-phosphatidylinositol. Whereas GPC3 is rich in foetal liver, its expression is barely measurable in adult liver [33]. In the present study, we found a significant increase in GPC3 mRNA expression in the DENA, DENA/galangin/luteolin, and DENA/DOX groups compared with the control group. In addition, the GPC3 mRNA expression was significantly decreased in the galangin/luteolin /DOX group compared with the DENA, DENA/galangin/luteolin, and DENA/DOX groups. These results are in agreement with a study which reported that GPC3 was overexpressed in HCC and that GPC3 expression level was a promising prognostic biomarker. In addition, GPC3 may also be a hopeful molecular target for the improvement of innovative therapies to enhance prognosis in patients with HCC [33]. Similarly to the

present study, a report by Min Yao *et al*. revealed that the GPC3 expression exhibited a gradual increase from non-malignant to malignant tissues, with brown granule-like staining focused in the neoplastic parts of lesions with atypical hyperplasia and in HCC [34].

HSPs are a large family of chaperones involved in protein folding and maturation of an assortment of client proteins, protecting these proteins from degradation, thermal stress, and oxidative stress [35]. Our results showed the increased expression of HSPs in the DENA, DENA/galangin/luteolin, and DENA/DOX groups compared with the control group. Furthermore, the expression of HSPs was significantly decreased after the combination treatment with galangin, luteolin, and DOX compared with the DENA group. These results are in agreement with a study which reported that the serum HSPs levels were markedly higher in patients with HCC and those with other cancers compared with controls. Additionally, upregulation of HSPs has been proposed as a prognostic and diagnostic marker in HCC [36].

In the present study, the hepatic tissue GSH and SOD content was significantly decreased in the DENA group ($p < 0.001$) compared with the control group. Furthermore, we observed significant decreases in the hepatic tissue GSH ($p < 0.001$) and SOD content ($p < 0.05$) in the DENA group treated with the combination of galangin, luteolin, and DOX in comparison to the control group, and a significant increase in the hepatic tissue GSH content ($p < 0.001$) in comparison to the DENA and DENA/galangin/luteolin groups, respectively, and a significant increase in the SOD content ($p < 0.001$) in comparison to DENA, DENA/galangin/luteolin, and DENA/DOXO groups, respectively.

There was also a significant increase in the hepatic tissue NO and MDA content in the DENA group ($p < 0.001$) compared with the control group. Similarly, significant increases in the hepatic tissue NO ($p < 0.001$) and MDA ($p < 0.05$) content were detected in the DENA group treated with galangin and luteolin in combination with DOX compared with the control group. Additionally, significant decreases ($p < 0.001$) in the hepatic tissue NO and MDA content were observed in comparison with the DENA, DENA/galangin/

luteolin, and DENA/DOX groups, respectively. These results are in line with a study which reported that both oxidative stress and free radicals are main players in cancer progression [37]. Additionally, increased generation of reactive oxygen species (ROS) and reductions in the levels of antioxidant enzymes in hepatic tissues have been reported in models of DENA-induced HCC [38]. Similarly, our findings are in agreement with a study which reported that the accumulation of ROS was an important contributing factor for apoptosis in many cancer cell types; the study also showed that the treatment with galangin improved intracellular ROS generation to prevent cancer cell proliferation, whereas blocking ROS accumulation suppressed galangin-induced apoptosis, suggesting that galangin-induced apoptosis is regulated by ROS. Additionally, the combination of phytochemical agents such as galangin and berberine resulted in ROS generation and apoptosis [29].

Our results have shown that the increase in the animal body weight was noticeably diminished in all (DENA + CCL4) animals during the sequence of the experiment before starting treatment. As illustrated in Figure 9, after treatments, the induced decreases in body weight gain were hindered to large extent in the combination group (DENA+DOX+L+G) and to less extent in (DENA+L+G) and (DENA+DOX).

As shown in Figure 10, livers from the DENA group showed abnormal morphological features with several macroscopic tumor nodules distributed throughout the liver with an irregular rough surface. Also, livers from rats treated with individual DOX and L+G macroscopically showed numerous scattered macro and micronodules of different sizes throughout the liver. On the contrary, livers in both the control and the combination group showed no tumor nodules.

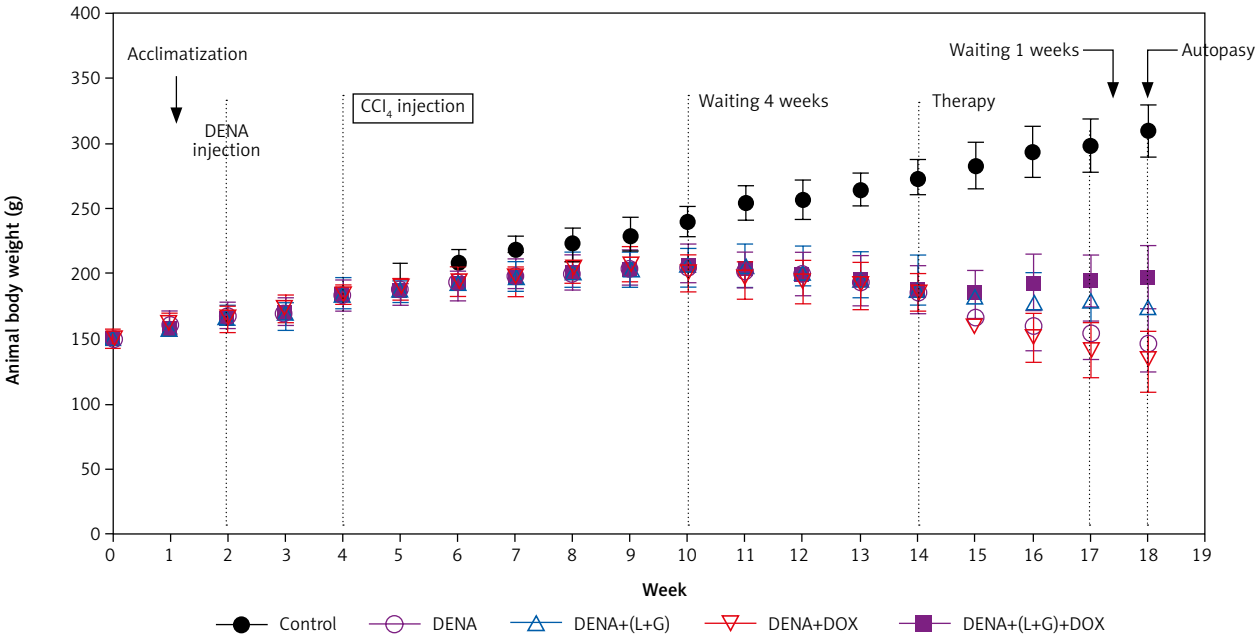

Fig. 9. Animal body weight

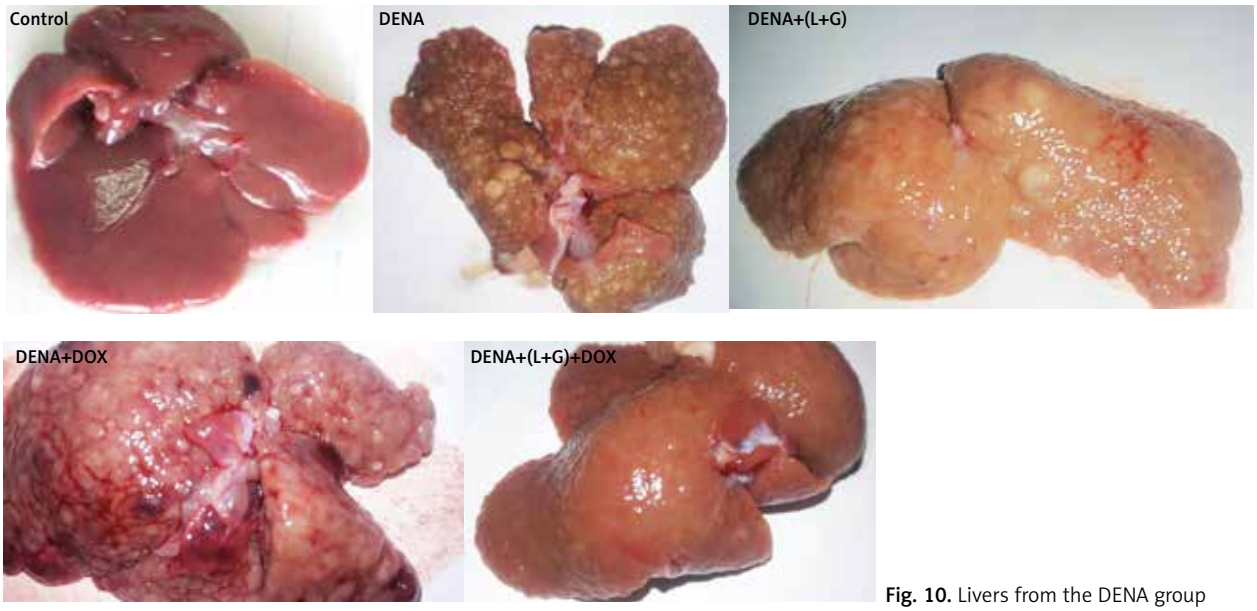

Fig. 10. Livers from the DENA group

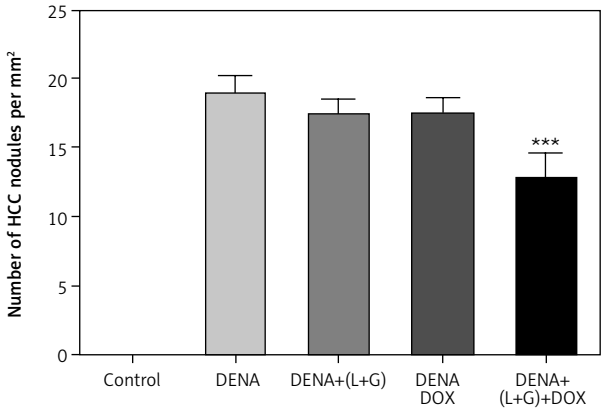

Fig. 11. Hepatocellular carcinoma nodules

The results revealed a significant increase in the number of HCC nodules in DENA, DENA+(L+G) and DENA+DOX in comparison to control group. Combination treatment consists of (galangin+luteolin+DOX) group showed a significant decrease in in the number of HCC nodules compared to DENA group as shown in Figure 11.

Conclusions

Both galangin and luteolin should be considered as potential candidates for clinical use in HCC chemotherapy, particularly as synergistic agents with DOX.

Acknowledgments

The authors are grateful to Assistant Prof. Dr. Walied sobhy, assistant professor of pathology Kafr El-Sheikh University, for carrying out the histopathological and immunohistochemical examinations.

The research procedures were performed in compliance with the National Institute for Animal Care Health Guidelines and approved by the Faculty of Pharmacy's Ethics Committee, Damanhur University (No. 117B24).

The authors declare no conflict of interests.

References

1. Bi W, Xiao J-Ch, Liuet R-J, et al. Identification of a 3,3-difluorinated tetrahydropyridinol compound as a novel antitumor agent for hepatocellular carcinoma acting via cell cycle arrest through disturbing CDK7-mediated phosphorylation of Cdc2. Invest New Drugs 2020; 38: 287-298.
2. Xu H, Yang T, Liu X, et al. Luteolin synergizes the antitumor effects of 5-fluorouracil against human hepatocellular carcinoma cells through apoptosis induction and metabolism. Life Sci 2016; 144: 138-147.
3. Yue QX, Liu X, Guo DA. Microtubule-binding natural products for cancer therapy. Planta Med 2010; 76: 1037-1043.
4. Zhu L, Luo Q, Bi J, et al. Galangin inhibits growth of human head and neck squamous carcinoma cells in vitro and in vivo. Chem Biol Interact 2014; 224: 149-156.
5. Sabry S, Ramadan A, Elghany M, et al. Formulation, characterization, and evaluation of the anti-tumor activity of nanosized galangin loaded niosomes on chemically induced hepatocellular carcinoma in rats. J Drug Deliv Sci Technol 2021; 61: 102163.
6. Murray TJ, Yang X, Sherr DH. Growth of a human mammary tumor cell line is blocked by galangin, a naturally occurring bioflavonoid, and is accompanied by down-regulation of cyclins D3, E, and A. Breast Cancer Res 2006; 8: 1-17.
7. Li F, Awale S, Tezuka Y, et al. Study on the constituents of Mexican propolis and their cytotoxic activity against PANC-1 human pancreatic cancer cells. J Nat Prod 2010; 73: 623-627.
8. Kim DA, Jeon YK, Nam MJ. Galangin induces apoptosis in gastric cancer cells via regulation of ubiquitin carboxy-terminal hydrolase isozyme L1 and glutathione S-transferase P. Food Chem Toxicol 2012; 50: 684-688.
9. Ha TK, Kim ME, Yoon JH, et al. Galangin induces human colon cancer cell death via the mitochondrial dysfunction and caspase-dependent pathway. Exp Biol Med (Maywood) 2013; 238: 1047-1054.
10. Chakrabarti M, Ray SK. Synergistic anti-tumor actions of luteolin and silibinin prevented cell migration and invasion and induced apoptosis in glioblastoma SNB19 cells and glioblastoma stem cells. Brain Res 2015; 1629: 85-93.
11. Jiang Y, Mackley H, Cheng H, et al. Anal carcinoma therapy: can we improve on 5-fluorouracil/mitomycin/radiotherapy? J Natl Compr Canc Netw 2010; 8: 135-144.
12. Dakshayani KB, Subramanian P, Manivasagam T, et al. Melatonin modulates the oxidant-antioxidant imbalance during N-nitrosodiethylamine induced hepatocarcinogenesis in rats. J Pharm Pharm Sci 2005; 8: 316-321.
13. Elsadek B, Mansour A, Saleem T, et al. The antitumor activity of a lactosaminated albumin conjugate of doxorubicin in a chemically induced hepatocellular carcinoma rat model compared to sorafenib. Dig Liver Dis 2017; 49: 213-222.
14. Wang X, Gong G, Yang W, et al. Antifibrotic activity of galangin, a novel function evaluated in animal liver fibrosis model. Environ Toxicol Pharmacol 2013; 36: 288-295.
15. Pandurangan AK, Kumar SAS, Dharmalingam P, Ganapasam S. Luteolin, a bioflavonoid inhibits azoxymethane-induced colon carcinogenesis: Involvement of iNOS and COX-2. Pharmacogn Mag 2014; 10: 306-310.
16. Livak KJ, Schmittgen TD. Analysis of relative gene expression data using real-time quantitative PCR and the 2(-Delta Delta C(T)) Method. Methods 2001; 25: 402-408.
17. Reitman S, Frankel S. A colorimetric method for the determination of serum glutamic oxalacetic and glutamic pyruvic transaminases. Am J Clin Pathol 1957; 28: 56-63.
18. Belfield A, Goldberg DM. Normal ranges and diagnostic value of serum 5'nucleotidase and alkaline phosphatase activities in infancy. Arch Dis Child 1971, 46: 842-846.
19. Walters MI, Gerarde H. An ultramicromethod for the determination of conjugated and total bilirubin in serum or plasma. Microchem J 1970; 15: 231-243.
20. Mihara M, Uchiyama M. Determination of malonaldehyde precursor in tissues by thiobarbituric acid test. Anal Biochem 1978; 86: 271-278.
21. Ellman GL. Tissue sulfhydryl groups. Arch Biochem Biophys 1959; 82: 70-77.
22. Sun L, Peterson TE, McCormick ML, Oberley LW, Osborne JW. Improved superoxide dismutase assay for clinical use. Clin Chem 1989; 35: 1265-1269.
23. Montgomery H, Dymock J. Determination of nitrite in water. Royal Soc Chemistry Thomas Graham House, Science Park, Milton Rd, Cambridge Cb4 0wf. J Med Lab Technol; 1961; 22: 111-118.
24. Rezvani G, Andisheh-Tadbir A, Ashraf MJ, et al. Evaluation of minichromosome maintenance-3 (MCM3) in oral squamous cell carcinoma. J Dent (Shiraz) 2015; 16: 87-92.
25. Leite AF, Bernardo VG, Buexm LA, et al. Immunoexpression of cleaved caspase-3 shows lower apoptotic area indices in lip carcinomas than in intraoral cancer. J Appl Oral Sci 2016; 24: 359-365.
26. Bancroft JD. Observations on the effect on histochemical reactions of different processing methods. J Med Lab Technol 1966; 23: 105-108.
27. 27. Zhang H, Li N, Wu J, et al. Galangin inhibits proliferation of HepG2 cells by activating AMPK via increasing the AMP/TAN ratio in a LKB1-independent manner. Eur J Pharmacol 2013; 718: 235-244.
28. Kessler SM, Leber B, Hoppstädter J, et al. Diethylnitrosamine (DENA) recapitulates formation of hepatic angiosarcoma in pigs. PLoS One 2019; 14: e0214756.

29. Ren K, Zhang W, Wu G, et al. Synergistic anti-cancer effects of galangin and berberine through apoptosis induction and proliferation inhibition in oesophageal carcinoma cells. Biomed Pharmacother 2016; 84: 1748-1759.
30. Imura S, Teraoku H, Yoshikawa M, et al. Potential predictive factors for microvascular invasion in hepatocellular carcinoma classified within the Milan criteria. Int J Clin Oncol 2018; 23: 98-103.
31. Wei T, Zhang W, Tan Q, Cui X, Dai Z. Electrochemical assay of the alpha fetoprotein-l3 isoform ratio to improve the diagnostic accuracy of hepatocellular carcinoma. Anal Chem 2018; 90: 13051-13058.
32. Chang J, Hsu J, Kuo P, Kuo Y, Chiang L, Lin Ch. Increase of Bax/ Bcl-XL ratio and arrest of cell cycle by luteolin in immortalized human hepatoma cell line. Life Sci 2005; 76: 1883-1893.
33. Haruyama Y, Kataoka H. Glypican-3 is a prognostic factor and an immunotherapeutic target in hepatocellular carcinoma. World J Gastroenterol 2016; 22: 275-283.
34. Yao M, Yao DF, Bian YZ, et al. Values of circulating GPC-3 mRNA and alpha-fetoprotein in detecting patients with hepatocellular carcinoma. Hepatobiliary Pancreat Dis Int 2013; 12: 171-179.
35. Chatterjee S, Burns TF. Targeting heat shock proteins in cancer: a promising therapeutic approach. Int J Mol Sci 2017; 18: 111-119.
36. Wang C, Zhang Y, Guo K, et al. Heat shock proteins in hepatocellular carcinoma: molecular mechanism and therapeutic potential. Int J Cancer 2016; 138: 1824-1834.
37. Prasad S, Gupta SC, Tyagi AK, Reactive oxygen species (ROS) and cancer: role of antioxidative nutraceuticals. Cancer Lett 2017; 387: 95-105.
38. Fu N, Yao H, Nan Y, Qiao L. Role of oxidative stress in hepatitis C virus induced hepatocellular carcinoma. Curr Cancer Drug Targets 2017; 17: 498-504.

Address for correspondence

Tarek Okda PhD
Department of Biochemistry
Faculty of Pharmacy
Damanhur University
Damanhur, Egypt
e-mail: tarekokda@yahoo.com

Submitted: 15.06.2021
Accepted: 02.08.2021